New Journal of Physics
The open-access journal for physics

Ultra-high-energy cosmic rays from black hole jets of radio galaxies

C D Dermer[1,3], S Razzaque[1,4], J D Finke[1,4] and A Atoyan[2]

[1] Code 7653, Naval Research Laboratory, Washington, DC 20375-5352, USA
[2] Concordia University, Montréal, Quebec H3G 1M8, Canada
E-mail: charles.dermer@nrl.navy.mil

New Journal of Physics **11** (2009) 065016 (20pp)
Received 7 November 2008
Published 30 June 2009
Online at http://www.njp.org/
doi:10.1088/1367-2630/11/6/065016

Abstract. The Auger Collaboration reports (Auger Collaboration 2007 *Science* **318** 939, The Pierre Auger Collaboration 2008 *Astropart. Phys.* **29** 188) that the arrival directions of $\gtrsim$60 EeV ultra-high-energy cosmic rays (UHECRs) cluster along the supergalactic plane and correlate with active galactic nuclei (AGN) within $\approx$100 Mpc. The association of several events with the nearby radio galaxy Centaurus A supports the paradigm that UHECRs are powered by supermassive black-hole engines and accelerated to ultra-high energies in the shocks formed by variable plasma winds in the inner jets of radio galaxies. The GZK horizon length of 75 EeV UHECR protons is $\approx$100 Mpc, so that the Auger results are consistent with an assumed proton composition of the UHECRs. In this scenario, the sources of UHECRs are FR II radio galaxies and FR I galaxies like Cen A with scattered radiation fields that enhance UHECR neutral-beam production. Radio galaxies with jets pointed away from us can still be observed as UHECR sources due to deflection of UHECRs by magnetic fields in the radio lobes of these galaxies. A broadband $\sim$1 MeV–10 EeV radiation component in the spectra of blazar AGN is formed by UHECR-induced cascade radiation in the extragalactic background light. This emission is too faint to be seen from Cen A, but could be detected from more luminous blazars.

[3] Author to whom any correspondence should be addressed.
[4] Naval Research Laboratory/National Research Council Resident Research Associate.

Contents

1. Introduction

The Auger Observatory in the Mendoza Province of Argentina at ≈36°S latitude determines the arrival directions and energies of ultra-high-energy cosmic rays (UHECRs) using four telescope arrays to measure Ni air fluorescence and 1600 surface detectors spaced 1.5 km apart to measure muons formed in cosmic-ray-induced showers. Event reconstruction using the hybrid technique gives arrival directions better than 1°, and energy uncertainties at 10^{20} eV (100 EeV) of ∼11% for a 50% Fe and 50% p composition [3]. The analysis of the composition of the high energy showers in the early Auger analysis showed them becoming heavier, somewhere between p and Fe, at $10^{19.4}$ eV [4, 5]. By contrast, HiRes data are consistent with dominant proton composition at these energies [6], but uncertainties in the shower properties [7] and particle physics extrapolated to this extreme energy scale [8] preclude definite statements about the composition.

In the Auger analysis [1, 2], a probability statistic P corrected for exposure is constructed from the nearest-neighbor angular separation ψ between the arrival direction of an UHECR with energy E and the directions to active galactic model (AGN) in the Véron-Cetty and Véron (VCV) catalog [9], containing 694 active galaxies with $z < 0.024$ or distance $d < 100$ Mpc. P was minimized for $\psi = 3.1°$, threshold clustering energy $E_{\rm cl} = 56$ EeV, and clustering redshift $z_{\rm cl} = 0.018$ ($d_{\rm cl} \cong 75$ Mpc), containing 27 events (the two highest energy events were 90 and 148 EeV). Twelve events correlate within 3.1° of the selected $d < 75$ Mpc AGN, and another three within the vicinity of one of these nearby AGN, ruling out an isotropic UHECR flux or a galactic source population. Note that the VCV AGNs are not necessarily the sources of the UHECRs, but may only trace the same matter distribution as the actual UHECR sources.

This discovery opens the field of charged-particle astronomy. Only at the highest energies can arrival directions of charged particles be associated with their sources. This is because deflections by (i) the galactic or (ii) intergalactic magnetic (IGM) field isotropizes the directions of lower energy cosmic rays.

Here we consider the Auger clustering results within the paradigm that extragalactic black-hole jet sources accelerate UHECRs. Estimates of deflection angle and delays are given in section 2, specialized to an assumed proton composition of the UHECRs. The question of the GZK cutoff and the UHECR horizon is revisited in section 3. In section 4, we apply standard synchrotron theory to the lobes of Cen A in order to estimate the equipartition magnetic field and absolute jet power, using a new technique that uses the jet/counter-jet ratio to determine the speed of the outflow. From this, limits on UHECR acceleration in colliding shells of blazars are used to derive maximum particle energies. Also, an estimate is made of the flux of Compton-scattered cosmic microwave (blackbody) background radiation (CMBR), and compared with the flux of secondary nuclear production in Cen A's radio lobes. In section 5, we present calculations of the broadband γ-ray νF_ν flux from Cen A due to secondary cascading of protons on the extragalactic background light (EBL) for 1 nG ($= 10^{-9}$ G) IGM fields, and show that Cen A is not detectable with current instrumentation. Concluding remarks are given in section 6.

2. Magnetic field deflections of UHECRs

For case (i), the galactic magnetic field can be approximated by a magnetic disk with characteristic height $h_{\rm md}$, giving a deflection angle $\theta_{\rm dfl} \approx h_{\rm md}\,{\rm cosec}\,b/r_{\rm L}$. Here b is the galactic latitude of the UHECR source, and the Larmor radius of a particle with energy E and charge Ze is

$$r_{\rm L} \cong 65\,\frac{(E/60\,{\rm EeV})}{ZB(\mu{\rm G})}\,{\rm kpc}\,. \tag{1}$$

Thus

$$\theta_{\rm dfl,MW} \lesssim 1^\circ\,\frac{Zh_{\rm md}({\rm kpc})B(\mu{\rm G})}{\sin\,b(E/60\,{\rm EeV})}\,, \tag{2}$$

limited by the finite extent of the magnetic disk. Mean magnetic fields B in the $\approx$0.2 kpc thick gaseous disk of the galaxy are $\approx$3–5 μG, but could fall to $\ll$1 μG in the kpc-scale halo [10]. Deflection angles $\lesssim 3^\circ$ from Cen A ($b = 19.4^\circ$, galactic longitude $\ell = 309.5^\circ$, declination -43°, distance $d \cong 3.5$ Mpc) restrict UHECRs to protons or light-Z nuclei and a small ($\lesssim$0.1 μG) galactic halo magnetic field.

For case (ii), the deflection angle of an UHECR ion when propagating through the IGM field from a source at distance d is [11, 12] $\theta_{d,{\rm IGM}} \simeq d/2r_{\rm L}\sqrt{N_{\rm inv}} \simeq 0.04^\circ\,Z\,\langle B_{-12}\rangle\,d(100\,{\rm Mpc})/[E(60\,{\rm EeV})\sqrt{N_{\rm inv}}]$, where $N_{\rm inv} \simeq \max(d/\lambda, 1)$ is the number of reversals of the magnetic field (also expressed through the magnetic-field correlation length λ) and $\langle B_{-12}\rangle$ is the mean magnetic field of the IGM in pico-Gauss (1 pG $= 10^{-12}$ G). If UHECRs within 3° of Cen A are accelerated by the radio jets of Centaurus A, then to avoid much larger deflections than those made by the galactic magnetic field requires that $\langle B_{-12}\rangle \lesssim 2000\,\sqrt{N_{\rm inv}}\,E(60\,{\rm EeV})/[Zd(3.5\,{\rm Mpc})]$. By this reasoning, the mean IGM field in the directions towards AGNs 75 Mpc distant in the supergalactic plane (SGP) is restricted to be $\lesssim 100\sqrt{N_{\rm inv}}\,E(60\,{\rm EeV})/Z$ pG [13]. Time delays between electromagnetic outbursts and UHECR arrival windows from Cen A due to propagation through the IGM are about

$$\Delta t \approx \frac{d^3}{24r_{\rm L}^2cN_{\rm inv}^{3/2}} \lesssim 0.5\,\frac{d^3(3.5\,{\rm Mpc})Z^2\langle B_{-12}\rangle^2}{E^2(60\,{\rm EeV})}\,{\rm day}\,, \tag{3}$$

where the final expression holds because $N_{\rm inv} \gtrsim 1$. Variable γ-ray flaring activity from Cen A could be reflected in variable UHECR activity on sub-day timescales for IGM fields $\langle B_{-12}\rangle \lesssim 10$ and $\lambda \lesssim 0.1$ Mpc or a large-scale (∼Mpc) ordered field with mean strength $\langle B_{-12}\rangle \lesssim 1$.

The most intense magnetic fields between us and Cen A, consistent with the deflection data for an assumed proton composition of the UHECRs, are $\langle B\rangle \approx 2\sqrt{N_{\rm inv}}$ nG. For the Auger data reaching galaxies at distance $d \gtrsim 75$ Mpc, $\langle B\rangle \lesssim 100\sqrt{N_{\rm inv}}$ pG. For $N_{\rm inv} \sim 100$ ($\lambda \cong 1$ Mpc), $\langle B\rangle \approx 1$ nG. For the calculations in section 5, we use $\langle B\rangle = 1$ nG, which is a more realistic value because UHECRs are correlated with more distant sources as well.

3. UHECR proton horizon

The clustering energy $E_{\rm cl} \cong 60$ EeV separates UHECRs formed mainly by sources along the SGP at $d \lesssim d_{\rm cl}$ from lower-energy UHECRs formed nearby and on $\gtrsim$75 Mpc scales. A high significant steepening in the UHECR spectrum at $E \cong 10^{19.6}$ eV $\cong 4\times 10^{19}$ eV and at $E \cong 10^{19.8}$ eV $\cong 6\times 10^{19}$ eV was reported, respectively, by the Auger [4] and HiRes [14] collaborations in 2007. These results confirm the prediction of Greisen [15] and Zatsepin and Kuzmin [16] that interactions of UHECRs with CMBR photons cause a break in the UHECR spectral intensity near 10^{20} eV.

The clustering and GZK energies coincide because $\gtrsim$60 EeV UHECR protons originating from sources at the $\gtrsim$100 Mpc scale have lost a significant fraction of their energy due to photopion losses with the CMBR, so that higher-energy particles from the more distant universe cannot reach us. The energy-loss mean free path $r_{\phi\pi} = ct_{\phi\pi} = c\gamma|{\rm d}\gamma/{\rm d}t|^{-1}_{\phi\pi}$ of an UHECR proton with energy $E = 10^{20}E_{20}$ eV to photopion losses with the CMBR at low redshifts is given, in good agreement with numerical calculations [17, 23], by the expression

$$r_{\phi\pi}(E_{20}) \cong \frac{13.7\exp[4/E_{20}]}{[1+4/E_{20}]}\,{\rm Mpc} \tag{4}$$

[13]. The term $r_{\phi\pi}$ gives the mean distance over which a particle with energy E loses $\approx 1-{\rm e}^{-1} \cong 63\%$ of its energy. The mean-free paths (MFPs) for energy loss by photopair and photopion losses in different model EBLs, including an EBL consisting of the CMBR alone, is shown in figure 1.

The GZK horizon length giving the mean distance from which protons detected with energy $10^{20}E_{20}$ eV originate depends, in general, on injection spectra and source evolution [18] (see also [19, 20]), but a model-independent definition that reduces to $r_{\phi\pi}(E_{20})$ for an energy-independent energy-loss rate considers the average distance from which a proton with measured energy E had energy eE. The horizon distance, defined this way, is given by

$$\begin{aligned} r_{\rm hrz}(E_{20}) &= \int_{E_{20}}^{eE_{20}} \frac{{\rm d}x}{x} r_{\phi\pi}(x) \\ &\cong 13.7\int_{E_{20}}^{eE_{20}} {\rm d}x\,\frac{\exp(4/x)}{x(1+4/x)}\,{\rm Mpc} \cong \frac{1.1E_{20}^2\exp(4/E_{20})}{1+1.6E_{20}^2/13.7}\,{\rm Mpc}, \end{aligned} \tag{5}$$

where the last two expressions give the proton horizon on CMBR photons alone.

The phenomenological fits to low and high EBLs at optical and IR frequencies, represented in the inset to figure 1 as a superposition of blackbodies [13], give the corrected horizon distance

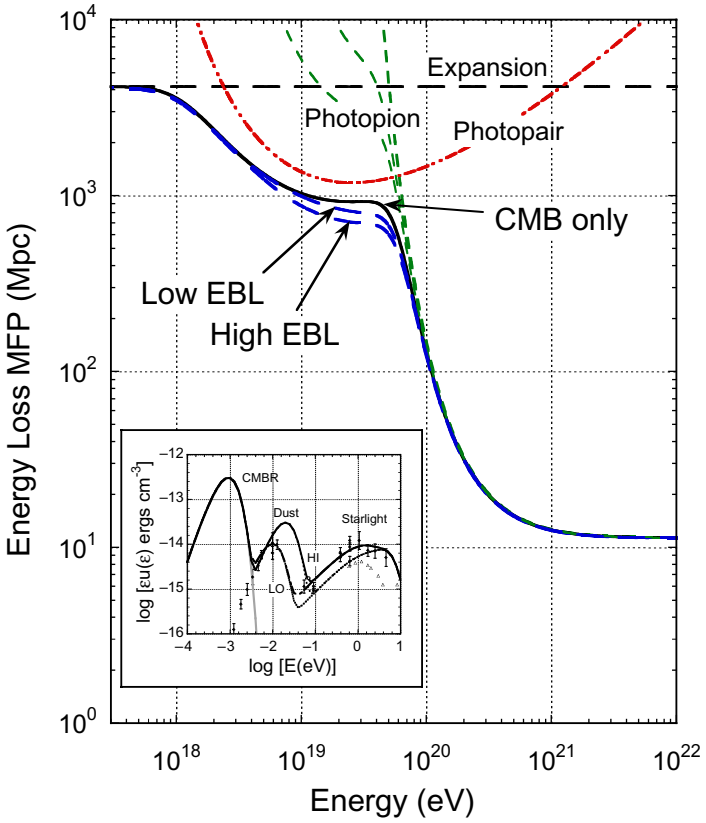

Figure 1. MFPs for energy loss of UHECR protons in different model EBLs are shown by the solid curves, with photopair (dotted) and photopion (dashed) components shown separately. 'CMB only' refers to total energy losses with CMB photons only. Inset: measurements of the EBL at optical and infrared frequencies, including phenomenological fits to low-redshift EBL in terms of a superposition of modified blackbodies. A Hubble constant of 72 km s^{-1} Mpc^{-1} is used throughout.

shown in figure 2. The horizon distance for ≈57 (75) EeV UHECR protons is ≈200 (100) Mpc. A GZK horizon smaller than 40 Mpc applies to protons with $E \gtrsim 100$ EeV. This explains the clustering observations observed by the Auger collaboration if UHECRs are predominantly protons, but would be inconsistent with the Auger results if the UHECRs are composed of high-Z material, as the MFP for photodisintegration can be much larger than 100 Mpc for $\approx 10^{20}$ eV ions such as Fe [13]. If the Auger energy scale is underestimated by ≈20% due to systematic effects (which would also reconcile the discrepancy between the different HiRes and Auger GZK energies as determined from the spectral break), then GZK losses on UHECRs with a dominant proton composition would explain the clustering towards the SGP even more decisively. The higher energy scale for the Auger experiment might also explain the lack of clustering observed by HiRes at >57 EeV [21], which would, at this energy cut in the HiRes experiment, include large numbers of lower-energy, more distant and less clustered cosmic rays.

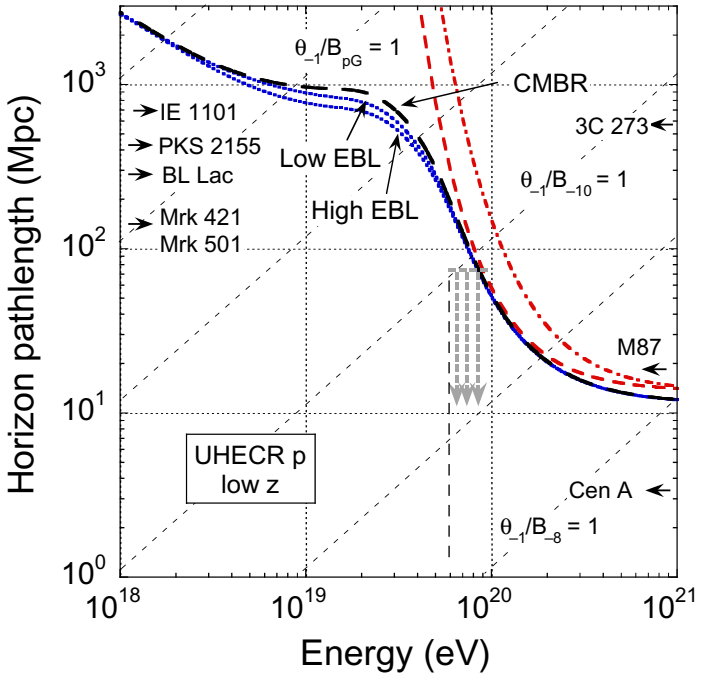

Figure 2. Heavy dotted curves give the horizon distance for UHECR protons as a function of total proton energy, using the local CMBR and the low and high EBL target radiation field shown in the inset to figure 1. Analytic approximation to photopion energy loss MFP, equation (4), is given by dot-dashed curve, and the UHECR proton horizon, equation (5), by dashed curve, for CMBR only. Auger clustering results are indicated by the shaded arrows. Distances to key radio galaxies are shown, and light dashed lines separate quasi-linear proton trajectories from trajectories with strong deflections in overall ordered magnetic fields with strength as labeled. Short-dashed lines give length for a proton to be deflected by $0.1\theta_{-1}$ rad in magnetic fields ranging from 10^{-8} to 10^{-11} G.

4. UHECRs from AGN jets

Discovery of UHECR arrival directions clustered towards the SGP was anticipated by analysis of UHECR data from Haverah Park, AGASA, Volcano Ranch, and Yakutsk observatories [22]; see also [23]. Compared to an isotropic source flux, the average and rms angular distances toward the SGP were enhanced at the 2.5–2.8σ level for events with $E > 40$ EeV. Stanev *et al* [22] argued that their analysis favors radio galaxies as the sources of UHECRs. A radio-galaxy origin of UHECRs is consistent with harder radio sources [24] and clustering of sources in the two Jansky, 2.7 GHz Wall and Peacock catalog [25] towards the SGP.

The SGP runs through the Virgo Cluster at ≈20 Mpc, and contains an assortment of radio galaxies such as M87, Cen A, and NGC 315, and the starburst galaxies M82 and NGC 253. Using infrared galaxy surveys to better define the SGP improves the significance of correlations of UHECRs with the SGP [26]. When weighted by hard x-ray flux, the UHECR arrival directions are strongly correlated with Swift Burst Alert Telescope galaxies within 100 Mpc, which trace the SGP [27]. Searches [28, 29] for specific AGN in the VCV and NASA/IPAC

NED catalogs finds Seyfert 2, low ionization, and other radio-quiet galaxies closest to the UHECR arrival directions, in addition to associations with Cen A, Cen B, an FR II radio galaxy, and a BL Lac object within 140 Mpc. IGR J21247 + 5058, an FR II broad-lined radio galaxy at $z = 0.02$ or $d \approx 80$ Mpc, recently discovered with INTEGRAL [30], is 2.1° away from a HiRes Stereo event with $E > 56$ EeV [31]. At least 8 of the 27 UHECRs with $E > 56$ EeV are within 3.5° of nearby radio galaxies [32].

We suppose that the evidence is compatible with an AGN origin of UHECRs in the black-hole jets of radio galaxies, with Centaurus A being the most prominent example. Cen A itself, though classified as an FR I radio galaxy, has a bolometric radio luminosity exceeding 4×10^{41} erg s^{-1} [33], near the dividing line between FR I and FR II galaxies in terms of radio power. The giant elliptical galaxy in Cen A is intercepted by a small spiral galaxy making the prominent dust lanes [34], which, including inner dust torus emission, could conceal the optical/UV line strengths and the distribution of broad line region gas near the Cen A nucleus [35, 36]. A strong scattered radiation field is important for photomeson losses and neutral beam production in AGN jets [37, 38], and seems required in many BL Lac objects because of spectral fitting difficulties with synchrotron/SSC models [39]–[41].

The nucleus of the Cen A jet is visible at radio and x-ray energies, revealing sub-luminal ($v \sim c/2$) relativistic outflows and jet/counterjet fluxes of x-ray knots consistent with mildly relativistic speeds on projected ∼10 pc scales [42, 43]. Cen A was detected at hard x-ray and γ-ray energies with OSSE, COMPTEL and EGRET on the *Compton Observatory* [44, 45], emitting $\approx 5 \times 10^{42}$ erg s^{-1} in keV–MeV radiation with day-scale variability observed at ≈100 keV (see also [46]). Most of this emission is probably quasi-isotropic radiation from the hot accretion plasma. Variability of ∼GeV radiation could be detected from Cen A with the *Fermi Gamma ray Space Telescope* if the jetted γ-ray emission is not too dim. Such a detection would also discriminate between an inner jet and extended origin of the γ-ray emission, for example, from Cen A's lobes [47].

4.1. Jet power from synchrotron theory

The corrected Auger point source exposure is $\chi\omega(\delta_s)/\Omega_{60} \cong (9000 \times 0.64/\pi)$ km^2 yr, where χ is the exposure, $\omega(\delta_s) \cong 0.64$ is an exposure correction factor for the declination of Cen A, and $\Omega_{60} \cong \pi$ is the Auger acceptance solid angle [48]. For a power law proton injection spectrum with number index α, the apparent isotropic UHECR luminosity from Cen A is

$$L_{\rm Cen\,A} \cong 1.6 \times 10^6 \times 60^{\alpha-1} \frac{4\pi d^2 N \Omega_{60}}{\chi\omega(\delta_s)} \left(\frac{\alpha-1}{\alpha-2}\right) [E({\rm EeV})]^{2-\alpha}\ {\rm erg\ s^{-1}}\,, \qquad (6)$$

which for $N = 2$ events gives $L_{\rm Cen\,A}(\alpha = 2.2) \simeq 5 \times 10^{39}[E({\rm EeV})]^{-0.2}$ erg s^{-1} and $L_{\rm Cen\,A}(\alpha = 2.7) \simeq 2 \times 10^{40}[E({\rm EeV})]^{-0.7}$ erg s^{-1}.[5] The Cen A radio luminosity thus greatly exceeds the UHECR luminosity unless cosmic rays are strongly beamed along the Cen A jet. The integrated cosmic ray power for $\alpha = 2.0$ from 1 GeV to 10^{20} eV is ≈2–3 $\times 10^{40}$ erg s^{-1} for $N = 5$ events.

It is interesting to note that the production of $\approx 10^{40}$ erg s^{-1} in UHECRs by Cen A, the dominant radio galaxy within ∼10 Mpc, represents an UHECR emissivity of $\simeq 8 \times 10^{43}$ erg yr^{-1} Mpc^{-3} (cf [49]).

[5] This power should be increased by a factor 2–3 if 5 or 6 events are associated with Cen A and its lobes [28].

4.1.1. Equipartition magnetic field. The UHECR luminosity can be compared with the time-averaged jet power inferred from the magnetic field energy in the radio lobes, assumed to be inflated by the pressure of the black-hole jet. Knowing the power of a black-hole jet allows one to derive the maximum particle energy of UHECRs accelerated through Fermi processes.

Here we state some elementary results from synchrotron theory needed to derive the jet power [50]. We treat a standard blob model and assume that the measured radio emission is nonthermal synchrotron radiation from randomly oriented electrons in a randomly directed magnetic field. In this approximation, the equipartition magnetic field is defined by equating the magnetic-field energy density $U_B = B^2/8\pi$ with the *total* particle energy density $U_{\rm par}$ consisting of hadrons and electrons, assumed to be dominated by a large-scale, randomly oriented magnetic field of strength B.

The equipartition magnetic field $B_{\rm eq} = B(k_{\rm eq} = 1)$ with $U_{\rm par} = k_{\rm eq} U_B$, where

$$B(k_{\rm eq}) = \frac{B_{\rm cr}}{\delta_{\rm D}} \left[\frac{3\pi d_L^2 m_{\rm e} c^2 f_{\epsilon_2}^{\rm syn} \ln(\epsilon_2/\epsilon_1)(1+\zeta_{\rm pe})}{V_b' c \sigma_{\rm T} U_{\rm cr}^2 k_{\rm eq} \sqrt{(1+z)\epsilon_2}} \right]^{2/7} . \tag{7}$$

Here $B_{\rm cr} = m_{\rm e}^2 c^3/e\hbar = 4.414 \times 10^{13}\,{\rm G}$, $U_{\rm cr} = B_{\rm cr}^2/8\pi = 7.752 \times 10^{25}\,{\rm erg\,cm^{-3}}$, and $\delta_{\rm D}$ is the Doppler factor. In this expression, a factor $\zeta_{\rm pe}$ more energy is assumed to be carried by protons and ions than leptons. This result applies to the $F_\nu \propto \nu^{-1/2}$ portion of the synchrotron spectrum made by electrons with $N'(\gamma') \propto \gamma'^{-2}$ that carry most of the energy.

The νF_ν synchrotron flux $f_\epsilon^{\rm syn}$ at photon frequency $\nu = m_{\rm e} c^2 \epsilon/h$ is found in equation (7). Note that $f_{\epsilon_2}^{\rm syn}/\sqrt{\epsilon_2}$ is constant throughout the range $\epsilon_1 \leqslant \epsilon < \epsilon_2$ when $f_\epsilon^{\rm syn} \propto \epsilon^{1/2}$, so that the value of $f_\epsilon^{\rm syn}/\sqrt{\epsilon}$ is independent of ϵ over this range. Also, $B_{\rm eq}$ depends only very weakly on the normalization of the energy contained in electrons, varying $\propto [\ln(\epsilon_2/\epsilon_1)]^{2/7}$.

4.1.2. Synchrotron power. The total jet power of a one-sided jet, referred to the stationary black-hole reference frame, is then

$$P_j^* \cong \pi r_b'^2 \beta c \Gamma^2 \left[\frac{B^2}{8\pi} + \frac{m_{\rm e} c^2 (1+\zeta_{\rm pe})}{V_b'} \frac{6\pi d_L^2 f_{\epsilon_2}^{\rm syn}}{2c\sigma_{\rm T} U_B \delta_{\rm D}^4} \sqrt{\frac{\delta_{\rm D} \varepsilon_B}{\epsilon_2 (1+z)}} \ln\left(\frac{\epsilon_2}{\epsilon_1}\right) \right] , \tag{8}$$

defining $\varepsilon_B = B/B_{\rm cr}$. From this, one can show [41, 50] that

$$P_j^*(B) = \frac{3}{7} P_j^*(B_{\min L}) \left(u^2 + \frac{4}{3u^{3/2}} \right) , \tag{9}$$

and $u \equiv B/B_{\min L}$. The minimum power is

$$P_j^*(B_{\min L}) = \frac{7}{3} \pi c \beta \Gamma^2 r_b'^2 U_{\rm cr} \left(\frac{B_{\min L}}{B_{\rm cr}} \right)^2 . \tag{10}$$

The magnetic field giving the minimum jet power required to account for the synchrotron flux is

$$B_{\min L} = \left(\frac{3}{4} \right)^{2/7} B_{\rm eq} \cong 0.921 B_{\rm eq} . \tag{11}$$

Table 1. Jet power of Cen A from synchrotron theory [a].

Regions [b]	F(Jy)	f_{-12}	ψ_0	g	β	$B_{\min L}$ (μG)	$\frac{P_j^*(B_{\min L})}{(\Gamma/\delta_D)^2(\lambda/10)^{4/7}}$ (10^{43} erg s^{-1})
1	91.2 ± 2.1	1.3	2.0	1	0.1	0.97	2.1
2	74.6 ± 3.0	1.5	1.0	1	0.2	0.99	3.4
3	545 ± 1.3	7.78	2.0	$\pi/6$		$1.96/\Gamma$	
4	204.7 ± 4.3	2.92	1.7	1	0.2	1.26	6.2
5	111.2 ± 6	1.59	1.6	1	0.1	1.08	2.2
Total	1026.7 ± 8.3	14.6					

[a]Radio observations at 21 cm from [47].
[b]Regions defined in [47].

4.1.3. Application to Centaurus A. The distance to Cen A is $d_{\mathrm{Cen}A} = 3.5 d_{3.5}$ Mpc, with $d_{3.5} \cong 1$. The preceding relations give

$$P_j^*(B_{\min L}) = \frac{7}{3}\pi c\beta \left(\frac{\Gamma}{\delta_D}\right)^2 r_b'^2 U_{\mathrm{cr}} \left[\frac{27 d_L^2 m_e c^2 f_{\epsilon_2}^{\mathrm{syn}} \ln(\epsilon_2/\epsilon_1)(1+\zeta_{\mathrm{pe}})}{16 c\sigma_T U_{\mathrm{cr}}^2 \sqrt{(1+z)\epsilon_2}}\right]^{2/7} . \quad (12)$$

This applies to either spherical or cubical volumes by writing the emitting volume in the fluid frame as

$$V_b' = g d_b'^3 = 6.7 \times 10^{69} g (d_{3.5}\psi_0)^3 \ \mathrm{cm}^3 . \quad (13)$$

The geometry factor is given by $g = 1$ for cubical and $g = \pi/6$ for spherical volumes. The angle ψ_0, in degrees, is the angular extent of the emitting volume.

Writing $f_\epsilon^{\mathrm{syn}} = f_{\epsilon_2}\sqrt{\epsilon/\epsilon_2}$, with $f_{\epsilon_2} = 10^{-12} f_{-12}$ erg cm^{-2} s^{-1}, and normalizing to the 21 cm (1.43 GHz) flux, so that $\epsilon_2 \cong 1.15 \times 10^{-11}\tilde{\epsilon}_{21}$, the magnetic field associated with the minimum jet power is

$$B_{\min L} = \frac{0.57}{\delta_D} \left(\frac{f_{-12}}{d_{3.5} g \psi_0^3}\right)^{2/7} \left(\frac{\ln(\epsilon_2/\epsilon_1)(1+\zeta_{\mathrm{pe}})}{\sqrt{\tilde{\epsilon}_{21}(1+z)}}\right)^{2/7} \mu\mathrm{G} . \quad (14)$$

The minimum jet power for a one-sided jet is, therefore,

$$P_j^*(B_{\min L}) \cong 4 \times 10^{43} \beta \left(\frac{\Gamma}{\delta_D}\right)^2 g^{2/21} d_{3.5}^{10/7} \psi_0^{2/7} \left(\frac{\ln(\epsilon_2/\epsilon_1)(1+\zeta_{\mathrm{pe}})}{\sqrt{\tilde{\epsilon}_{21}(1+z)}}\right)^{4/7} \mathrm{erg\ s}^{-1}. \quad (15)$$

Taking the bolometric factor $\ln(\epsilon_2/\epsilon_1)(1+\zeta_{\mathrm{pe}}) = 10$ in equations (14) and (15) gives the results shown in table 1 for the five different regions defined in [47]. Uncertainties by a factor 10 in the bolometric factor translate to a factor $10^{2/7} \cong 1.93$ in $B_{\min L}$ and a factor $10^{4/7} \cong 3.73$ in $P_{\min L}$.

To get the speed of the outflow, we use the jet/counterjet ratio ρ, which is a number taken directly from observations. If θ is the angle of the jet nearest to the line of sight, and we assume that all jets are two-sided with equal power ejected in the opposite direction, then it is easy to show [51, 52] that the speed

$$\beta c = \frac{c}{\cos\theta} \left(\frac{\rho^{2/7} - 1}{\rho^{2/7} + 1}\right) . \quad (16)$$

Thus we interpret the asymmetrical lobe flux in Cen A as a consequence of aberration of the mildly relativistic two-sided outflow, rather than as a difference of spectral properties due to distinct environmental effects. The jet power obtained from this interpretation can be compared with other methods to determine jet power [53].

Table 1 shows the jet/counterjet ratio $\rho \approx 1.5$–2 for regions 1 and 5, and $\rho \approx 2$–4 for regions 2 and 4, each pair being at equal angular separation from Cen A's nucleus. The orientation θ of the jet of Cen A with respect to our line of sight is $35^\circ \lesssim \theta \lesssim 72^\circ$ [54], implying that $\beta \approx 0.1$ for regions 1 and 5, and $\beta \approx 0.2$ for regions 2 and 3, which are the values used in the calculations of the jet power shown in table 1. These speeds refer to the flow of plasma on the scale of hundreds of kpc from the nucleus of Cen A, so that the plasma from the inner jet has to be ejected with much higher, probably relativistic speeds. The factor $(\Gamma/\delta_{\rm D})^2$, when included, reduces the power of the brighter lobe and increases the power of the dimmer lobe to reproduce the underlying assumption in the method that the powers of the two jets are equal. The minimum total jet power to produce the weakly boosted Cen A radio emission is therefore $\approx 2 \times 4 \times 10^{43}\,{\rm erg\,s^{-1}}$, or total jet power $P_*^{\rm tot} \gtrsim 10^{44}\,{\rm erg\,s^{-1}}$, as follows from table 1.

With total mean absolute Cen A jet powers $\approx 10^{44}\,{\rm erg\,s^{-1}}$, apparent isotropic jet powers can reach 10^{45}–$10^{46}\,{\rm erg\,s^{-1}}$ during flaring intervals. Indeed, apparent isotropic flaring luminosities in γ rays alone exceed $10^{45}\,{\rm erg\,s^{-1}}$ in Mrk 501 and Mrk 421, and $10^{46}\,{\rm erg\,s^{-1}}$ in PKS 2155-304 [55]. These AGN are nearby BL Lac objects that correspond to FR I radio galaxies such as Cen A seen along the jet axis, though Cen A may have the added advantage, in terms of UHECR production, of an external radiation field to enhance photohadronic processes in the jet [37, 38]. It will be interesting to apply this technique to a sample of radio galaxies, including Perseus A (3C 84, NGC 1275; $z = 0.018$ or $d_L \cong 76\,{\rm Mpc}$) [56, 57], Cyg A [31], etc.

4.2. UHECR acceleration

The particle energy density of a cold relativistic wind with apparent isotropic luminosity L and Lorentz factor $\Gamma = 1/\sqrt{1-\beta^2}$ at radius R from the source is $u_{\rm p} = L/(4\pi R^2 \beta \Gamma^2 c)$. If a fraction ϵ_B is channeled into magnetic field B' in the fluid frame, then $RB'\Gamma = \sqrt{2\epsilon_B L/\beta c}$, implying maximum particle energies $E'_{\rm max} \cong QB'(R/\beta\Gamma)$, so

$$E_{\rm max} \cong E'_{\rm max}\Gamma \cong \left(\frac{Ze}{\Gamma}\right)\sqrt{\frac{2\epsilon_B L}{\beta c}} \cong 2 \times 10^{20} Z \frac{\sqrt{\epsilon_B L/10^{46}\,{\rm erg\,s^{-1}}}}{\beta^{3/2}\Gamma}\,{\rm eV}\,. \qquad (17)$$

This simple, optimistic estimate begs the question of how to transform directed particle kinetic energy into magnetic field energy in a cold wind. In other words, it is simply a dimensional analysis that contains no physical basis, whether for the source that emits a wind with such large apparent powers, or for the particle acceleration mechanism.

Within the picture of particle acceleration through Fermi processes, a maximum particle energy in colliding shells can be derived in a straightforward manner. The underlying limitation of Fermi acceleration, whether first or second order, is that a particle cannot gain a significant fraction of its energy on a timescale shorter than the Larmor timescale. A colliding shell picture due to inhomogeneities in the relativistic wind realistically applies to the inner jets of radio galaxies and blazars, and to GRBs.

Consider the ejection of two shells, with shell a ejected at stationary frame times $0 \leqslant t_* < \Delta t_{*a}$, and shell b at times $t_{*d} \leqslant t_* < t_{*d} + \Delta t_{*b}$. The coasting Lorentz factor, wind luminosity (assumed constant during the duration of shell ejection), and energy are $\Gamma_{a(b)}$, $L_{*,a(b)}$ and $\mathcal{E}_{*,a(b)}$,

respectively, with stars referring to the stationary jet frame. For a collision, $\rho_\Gamma \equiv \Gamma_a/\Gamma_b < 1$. For relativistic winds i.e., $\Gamma_a \gg 1$, the collision radius is $r_{\rm coll} \cong 2\Gamma_a^2 c(t_{*d} - \Delta t_{*a})$ when $\rho_\Gamma \ll 1$. When $\Gamma_b > \Gamma_a \gg 1$, the shocked fluid Lorentz factor $\Gamma \gg 1$.

Collisions between relativistic shells divide into a number of cases depending on whether the forward shock (FS) and reverse shock (RS) are relativistic or nonrelativistic [58]. We consider the case of a nonrelativistic reverse shock (NRS) and relativistic forward shock (RFS), which is probably most favorable for particle acceleration. Thus the FS Lorentz factor $\Gamma_f \gg 1$. The magnetic field of the forward-shocked fluid in the shocked fluid (primed) frame is

$$B'_f = \frac{\Gamma_f}{r_{\rm coll}\Gamma_a}\sqrt{\frac{8\epsilon_{B,f}L_a}{c}} \tag{18}$$

and $\epsilon_{B,f}$, the ϵ_B parameter for the FS, is familiar from blast wave studies (e.g. [59]).

The maximum particle energy in the comoving frame is $E'_{\rm max} \cong ZeB'_{\rm f}c\Delta t'_a$, where $\Delta t'_a$ is the comoving duration when particles are undergoing acceleration. If this is equated with the time that it takes for the FS to pass through shell a, then

$$\Delta t'_a \cong \frac{\Gamma\Delta_a(r_{\rm coll})}{\Gamma_f c}\,. \tag{19}$$

From this, we obtain

$$E_{\rm max} = \Gamma E'_{\rm max} \cong \frac{Ze}{((t_{*d}/\Delta t_{*a}) - 1)}\,\frac{\Gamma}{\Gamma_a^2}\sqrt{\frac{2\epsilon_{Bf}L_a}{c}} \lesssim 2.4\times 10^{20} Z\,\frac{\Gamma}{\Gamma_a^2}\sqrt{\epsilon_{Bf}L_{46}}\,{\rm eV}. \tag{20}$$

The factor Γ/Γ_a^2 is at best of order unity, so this expression shows that for protons to reach $\gtrsim 10^{20}$ eV cosmic ray energies through Fermi processes, it is essential to consider sources with apparent isotropic luminosities $\gtrsim 10^{46}\,{\rm erg\,s^{-1}}$.

Acceleration of UHECRs in Cen A is therefore, in principle, possible during powerful episodes of jet activity. Acceleration of UHECRs can also take place in colliding winds of moderately powerful blazars with $L \gtrsim 10^{46}\,{\rm erg\,s^{-1}}$ where strong Doppler collimation takes place.

4.3. Deflection of UHECRs

The milliarcsec-scale radio jets in Cen A show moderate asymmetry, consistent with Cen A's radio jet being mildly relativistic and misaligned by $\sim 60^\circ$ [60]. Off-axis radiation beaming factors would conceal on-axis Cen A blazar-type flares with apparent powers $L \gtrsim 10^{46}\,{\rm erg\,s^{-1}}$. These events would eject cosmic rays to $\gtrsim 10^{20}$ eV energies into the $\sim$100 kpc $\times$ 500 kpc radio lobe structure. If the equipartition field characterizes the large-scale magnetic field of the lobes (i.e. $N_{\rm inv} \sim 1$), then 60 EeV UHECR protons with $r_{\rm L} \cong 65$ kpc (see equation (1)) could be deflected by the magnetic field of Cen A's lobe, or in the lobes of other radio galaxies or BL Lac objects, as suggested in arrival direction maps [28].

If UHECRs are formed through a neutron beam, then they will travel on average $\approx 500[E/(60\,{\rm EeV})]$ kpc before decaying. Thus UHECRs will be deposited throughout the radio lobe, with some not decaying until outside the radio lobe structure. Thus both radio galaxies and blazars can be the sources of UHECRs. For distant sources, though, energy losses will reduce the arrival energies of UHECRs, so that searches for enhancements of UHECRs towards specific sources should also take into account the EBL-dependent horizon energy, as illustrated in figure 2.

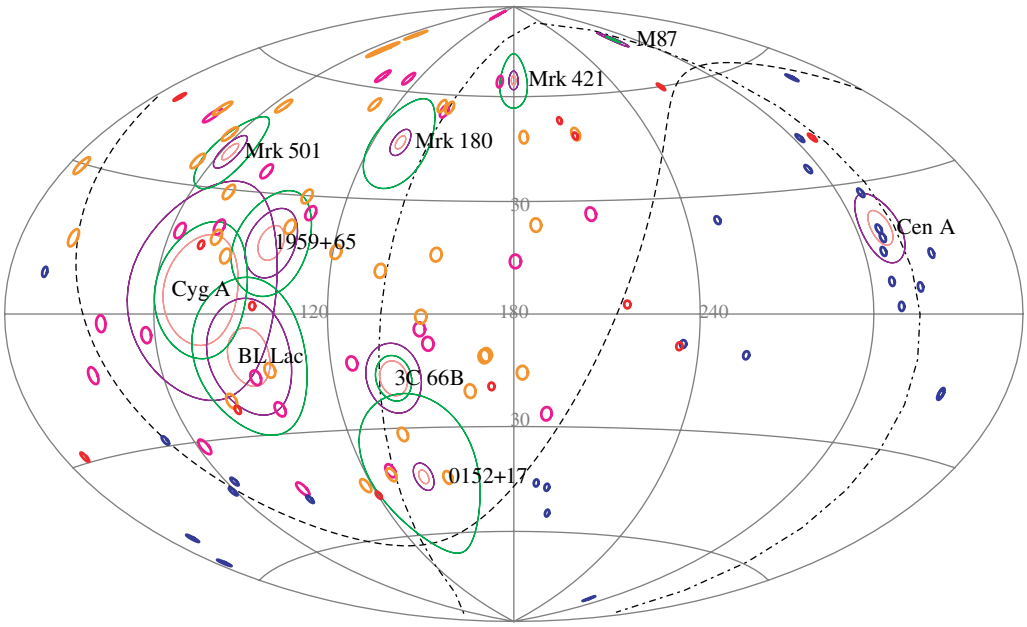

Figure 3. Hammer–Aitoff projection in galactic coordinates of UHECR arrival directions and directions to nearby prominent AGN; the direction to the galactic center is at the left and right extremities of this plot. Thick blue, red, and orange and magenta circles correspond to UHECRs with >56 EeV from Auger, >56 EeV from HiRes, and >40 EeV from AGASA, respectively. The radii of the circles reflect the angular errors in the reconstructed cosmic ray directions, which is 1° for both Auger and HiRes and 1.8° for AGASA. The centers of the concentric green, purple, and pink circles correspond to the named AGN directions. The pink and purple circles represent angular deflections from the source AGN of the arriving cosmic rays with 40 EeV and 20 EeV energies, respectively, in the μG galactic disk magnetic field, using equation (2). The green circles, on the other hand, represent angular deflection in an assumed 0.1 nG intergalactic magnetic field, assuming no magnetic-field reversals. The dashed and dot-dashed curves correspond to the equatorial and SGPs.

The proton Larmor radius is formally $r_{\rm L} \cong 110 E_{20}/B_{p\rm G}$ Gpc (equation (1)), and photomeson interactions with the CMBR and EBL take place on a horizon distance scale $\approx r_{\rm hor}(E_{20})$, where the received proton has lost ≈63% of its energy. If the proton is hardly deflected out of the beam, so $d \ll r_{\rm L}$, then we should expect a pulse pile-up at a specific energy $r_{\rm hor}(E_{20}) \cong d_{\rm L}$. For PKS 2155-304 at $z = 0.116$ or a propagation distance $d \cong 400$ Mpc (figure 2), searches should be made for enhancements of UHECRs with $E_{\rm CR} \lesssim 40$ EeV, which is insensitive to the level of the EBL. If BL Lac objects accelerate UHECRs, then enhancements at $E_{\rm CR} \sim 40$–60 EeV can be searched for from Mrk 421 and Mrk 501. Failure to detect a signal would constrain the minimum IGM field and number of inversions, or call into question a radio/γ-ray galaxy origin of UHECRs.

In figure 3, we plot the arrival directions of 27 cosmic rays from Auger (blue circles) and 13 cosmic rays from HiRes (red circles), all with >56 EeV energy and with 1° angular uncertainty in their arrival directions (reflected in the radii of the circles; cf [61]). We also plot the arrival

directions of 58 AGASA UHECRs, consisting of 24 with $E > 56$ EeV (magenta circles) and 34 with 40 EeV $< E <$ 56 EeV (orange circles). Their arrival directions are displayed with an average angular resolution of 1.8°, as previously reported by the AGASA experiment [62]. The number of AGASA UHECRs may suggest, given AGASA's exposure relative to HiRes and Auger, an energy calibration discrepancy between these experiments, which should be considered in more detailed studies but is ignored here. Note that the arrival directions of the cosmic rays from the prominent nearby AGNs (labeled) are deflected by the galactic (pink and purple circles) and inter-galactic (green circles) magnetic field. We used two energies, 40 EeV (pink circles) and 20 EeV (purple circles), to calculate deflections in the μG galactic magnetic field according to equation (2). The deflections from the AGN near the galactic plane (horizontal line) are larger because of the larger magnetic field.

If Cyg A, BL Lac, 1959 + 65, or Mrk 501 are the possible sources of UHECR, then we should expect a large scattering, due to the galactic magnetic field, in the arrival directions of UHECRs below the GZK energy. For distant sources, e.g. 0152 + 17, the deflection in the IGM field, plotted here for 0.1 nG field using green circles, may be larger. However, reversals of the field orientation over ∼ Mpc scale may reduce the deflection in the IGM field from the values plotted in figure 3. These deflections in magnetic fields and related uncertainties can prevent positive identification of the UHECR sources below the GZK energy, although one should expect a clustering effect as evident from the lower energy AGASA data in the northern hemisphere.

4.4. Nuclear γ rays from Cen A's radio lobes

Typical $\sim 1\mu$G magnetic fields in Cen A's lobes carry an amount of energy $\cong V_{\rm lobes} B^2/8\pi \cong 4 \times 10^{57} V_{71} B_{\mu\rm G}^2$ erg cm^{-3}, denoting the Cen A lobe volume $V_{\rm lobes} = 10^{71} V_{71}$ cm^{-3}. For magnetic fields near equipartition, only $\approx$ few Myr are required for a jet power of $\approx 10^{44}$ erg s^{-1} and a total energy of $\approx 10^{58}$ erg. Thus the Cen A jet activity is likely to operate intermittently.

Assuming at least equal energy in nonthermal protons and ions as nonthermal electrons, and using the equipartition assumption to normalize particle number and energy, we write the total cosmic ray spectrum over the Cen A lobes as

$$N_{\rm CR}(\gamma) = \frac{W_{\rm CR}}{m_p({\rm erg})} \frac{p-2}{1-\gamma_{\rm max}^{2-p}} \gamma^{-p}\,, \quad \text{for } 1 \lesssim \gamma \lesssim \gamma_{\rm max}\,, \tag{21}$$

with $\gamma_{\rm max} \sim 10^{11}$ and total cosmic-ray energy $W_{\rm CR} = 10^{58} W_{58}$ erg. A δ-function approximation for the inelastic nuclear cross section, $d\sigma_{pH\to\gamma}/dE_\gamma \cong 2\sigma_{\pi^0 X}(\gamma)\delta(E_\gamma - \xi E_p)$, where $\sigma_{\pi^0 X}(\gamma) \cong 27 \ln \gamma + 58/\sqrt{\gamma} - 41$ mb is the π^0 inclusive cross section [63] and γ-ray secondary fractional energy $\xi \sim 5$–10%, gives a lobe-integrated $\gtrsim 1$ GeV νF_ν spectrum

$$f_\epsilon^{pp\to\gamma} = \nu F_\nu^{pp\to\gamma} = \frac{\xi c n_\ell}{2\pi d^2} W_{\rm CR}(p-2)\sigma_{\pi^0}(\tilde\gamma), \quad \tilde\gamma \equiv \left(\frac{E_\gamma}{\xi m_p c^2}\right), \tag{22}$$

so

$$f_\epsilon^{pp\to\gamma}\ ({\rm erg\,cm^{-2}\,s^{-1}}) \simeq \frac{4\times 10^{-12}\xi^{p-1}(p-2)}{0.94^{2-p}} \left(\frac{n_\ell}{10^{-4}{\rm cm^{-3}}}\right) \times \frac{W_{58}}{d_{3.5}^2}\left[\frac{\sigma_{\pi^0 X}(E_\gamma/\xi m_p c^2)}{100\,{\rm mb}}\right] E_\gamma^{2-p}. \tag{23}$$

For $\xi = 0.05$ and $p \cong 2.3$, the nuclear γ-ray flux from the lobes of Cen A is

$$f_\epsilon^{pp\to\gamma} \simeq \frac{2.4\times10^{-14} W_{58} E_\gamma^{-0.3}}{d_{3.5}^2} \left(\frac{n_\ell}{10^{-4}\,\mathrm{cm}^{-3}}\right)\left[\frac{\sigma_{\pi^0 X}(20E_\gamma)}{100\,\mathrm{mb}}\right]\frac{\mathrm{erg}}{\mathrm{cm}^2\,\mathrm{s}}, \qquad (24)$$

with E_γ now in GeV. Based on lack of observed internal depolarization and measured soft x-ray flux, Hardcastle *et al* [47] argue that thermal particle target densities $n_\ell \sim 10^{-4}\,\mathrm{cm}^{-3}$.

The number of source counts with $E_\gamma(\mathrm{GeV}) \geqslant E_1$ detected with the Fermi Telescope for $\xi = 0.05$ and $p \cong 2.3$ is $S(>E_1) \cong X\Delta t f_{\mathrm{GeV}} \int_{E_1}^{\infty} \mathrm{d}E_\gamma E_\gamma^{a-2} A_{\mathrm{G}}(E_\gamma) \approx 0.7(X/0.2)\Delta t\,(\mathrm{yr})(n_\ell/10^{-4}\,\mathrm{cm}^{-3}) W_{58} E_\gamma^{-1.3}$, where the effective area of the Fermi Telescope is $A_{\mathrm{G}}(E_\gamma) \cong 8500/\sqrt{E_\gamma}\,\mathrm{cm}^2$ below 1 GeV and $A_{\mathrm{G}}(E_\gamma) \cong 8500\,\mathrm{cm}^2$ at higher energies, and $X \approx 1/5$ in the scanning mode. The number of background counts from the angular extent, $\Delta\Omega \cong 12/57.3^2$, of the lobes of Cen A, using as background the diffuse extragalactic γ-ray background of galactic background [64], is $B(>E_\gamma) \cong 280(X/0.2)\Delta t\,(\mathrm{yr}) E_\gamma^{-1.1}$.[6] Unless $n_\ell \gg 10^{-4}\,\mathrm{cm}^{-3}$, this emission signature would be too faint to be detected with the Fermi Gamma ray Space Telescope. Thus the cosmic-ray-induced nuclear emission in the lobes of Cen A is probably entirely negligible. The much more optimistic estimates in [65] are due to the assumption of a very soft injection index $p \cong 2.7$ extending from GeV to ZeV energies, which requires a much larger cosmic-ray power.

4.5. Thomson-scattered CMBR

The same electrons that make the radio synchrotron radiation also upscatter photons of the surrounding radiation fields. Using a δ-function approximation for Thomson scattering of quasi-monochromatic photons with mean energy $m_{\mathrm{e}}c^2\epsilon_0$ and energy density U_0 gives the Thomson-scattered νF_ν flux

$$f_\epsilon^{\mathrm{T}} \cong \delta_{\mathrm{D}}^2 \left(\frac{U_0}{U_B}\right) f_{\epsilon_{pk}}^{\mathrm{syn}} \sqrt{y} H(y;0,1), \quad y = \frac{\epsilon\varepsilon_B}{2\delta_{\mathrm{D}}\epsilon_0\epsilon_{pk}}; \qquad (25)$$

the value of the Heaviside function $H(y;0,1) = 1$ when $0 \leqslant y < 1$ and $H(y;0,1) = 0$ otherwise. For the CMBR, $m_{\mathrm{e}}c^2\epsilon_0 = 1.24\times10^{-9} m_{\mathrm{e}}c^2 = 0.63\,\mathrm{meV} = 153\,\mathrm{GHz}$ and $U_0 \cong 4\times10^{-13}(1+z)^4\,\mathrm{erg\,cm}^{-3}$ (recall that $\varepsilon_B = B/B_{\mathrm{cr}}$). Thus

$$f_\epsilon^{\mathrm{T}} \cong \frac{10\delta_{\mathrm{D}}^2}{B_{\mu\mathrm{G}}^2} f_{\epsilon_{pk}}^{\mathrm{syn}} \sqrt{\frac{\epsilon}{\epsilon_{\mathrm{T}}}}\, H(\epsilon;0,\epsilon_{\mathrm{T}})\,. \qquad (26)$$

For the CMBR, the mean dimensionless energy of a photon that is scattered by an electron radiating most of its synchrotron emission at ϵ_{pk} is

$$\epsilon_{\mathrm{T}} = \frac{2\delta_{\mathrm{D}}\epsilon_0\epsilon_{pk}}{\varepsilon_B}, \qquad (27)$$

implying emission at

$$E_{\mathrm{T}} \cong 43\frac{\delta_{\mathrm{D}}}{B_{\mu\mathrm{G}}}\left(\frac{\nu_{pk}}{100\,\mathrm{GHz}}\right)\mathrm{MeV}\,. \qquad (28)$$

The WMAP observations at 22.5, 32.7, 40.4, 60.1 and 92.9 GHz used by Hardcastle *et al* [47] allowed these authors to predict the Thomson-scattered flux. As can be seen from

[6] The galactic diffuse γ-ray background has a softer spectrum than the extragalactic background, so is probably not significant at $E_\gamma \gg 1$ GeV at the $\approx+20^\circ$ galactic latitude of Cen A.

this approximation, this flux extends only to the low-energy end ($\lesssim$100 MeV) of the Large Area Telescope frequency range on the Fermi Gamma ray Space Telescope [66].

5. Cascade γ rays from UHE neutral beams

For flares in BL Lacs exceeding $\gtrsim 10^{46}\,\mathrm{erg\,s^{-1}}$, and the much more energetic flares in FR II galaxies and flat-spectrum radio quasars reaching apparent γ-ray powers $\gtrsim 10^{48}\,\mathrm{erg\,s^{-1}}$, we describe the sequence of events starting to produce cascade radiation following the acceleration of particles in black-hole jets [38]. A neutral beam is formed as a consequence of photomeson interactions of the accelerated UHECR protons with the synchrotron and scattered radiation field in the inner jet. Some $\gtrsim$10% of the hadronic energy can be transformed into an escaping neutron beam, with a few per cent in a UHE γ-ray beam and a few per cent into neutrinos [37, 38]. Escaping neutrons with energy $E_{\rm n}$ travel $E_{\rm n}/10^{20}$ eV Mpc before decaying into protons and low-energy β-decay leptons and neutrinos.

The γ rays formed by $\mathrm{p,n}+\gamma\rightarrow\pi^0\rightarrow 2\gamma$ processes in the inner jet and particle beam are attenuated by CMBR photons through $\gamma\gamma\rightarrow \mathrm{e}^{\pm}$ on length scales $\lambda^{bb}_{\gamma\gamma}(\mathrm{kpc})\cong 2E_{\rm PeV}/\ln(0.4E_{\rm PeV})\,\mathrm{kpc}$ for $E_{\rm PeV}\gg 1$ and $\lambda^{bb}_{\gamma\gamma}(\mathrm{kpc})\cong 4\sqrt{E_{\rm PeV}}\exp(1/E_{\rm PeV})\,\mathrm{kpc}$ for $E_{\rm PeV}\ll 1$, valid until $E_{\rm PeV}<0.1$, when absorption on the EBL from stars and dust dominates. Leptons with $\gamma\equiv 10^9\gamma_9$ Compton-scatter the CMBR photons, losing energy on length scales $\lambda_{\rm T}\cong 0.75/\gamma_9\,\mathrm{kpc}$ when $\gamma_9\ll 1$, and $\lambda_{\rm KN}\cong 2.1\gamma_9/[\ln(1.8\gamma_9)-2]\,\mathrm{kpc}$ when $\gamma_9\gg 10$.

If the distance d to the source is smaller than the particle Larmor radius and the correlation length (formally, $N_{\rm inv}=1$), the cascade pairs are deflected out of a beam with opening angle $\theta=0.1\theta_{-1}$ rad when $\theta r_{\rm L}<\lambda_{\rm T}$, implying that the collimation of the electromagnetic cascade is preserved until $\gamma_9\cong 0.4\sqrt{B_{-11}/\theta_{-1}}$. Before the beam disperses, CMBR photons are scattered to energies $\epsilon\sim 10^{-9}\gamma^2$, or $E_\gamma\cong 100B_{-11}/\theta_{-1}$ TeV. Figure 4 shows that the ratio $B_{-11}/\theta_{-1}\lesssim 0.1$ is unique in that Compton-scattered CMBR from the cascade emerges from behind the EBL absorbing screen to form a hard γ-ray component at 10 GeV–10 TeV energies. If $B_{\rm IGM}\lesssim 10^{-12}$ G, then the cascade emission from sources such as 1ES 1101-232, if UHECR sources, could make an anomalous hard γ-ray component.

The high-energy cascade flux induced by rectilinear motions of UHECRs from Cen A towards us is shown in figure 5. This calculation is a one-zone model, because it assumes that the properties of the IGM remain unchanged between Cen A and the galaxy. Cosmic ray propagation through the extended magnetized environment in the cocoon and radio lobes of Cyg A [31] can also produce a γ-ray signature, but Cyg A is beyond the GZK horizon, so only lower energy UHECRs can reach us from this source. (For UHECRs accelerated in galaxy clusters [67] or other accelerators see e.g. [68].) This calculation is normalized to two protons from Cen A with $E>60$ EeV for the exposure and area of the Auger observatory (equation (6)).

The parameters of this calculation are $d=3.5$ Mpc, $B=10^{-9}$ G, and particle injection index $\alpha=2.2$. The proton injection spectrum is exponentially cutoff at energy $E_{\rm max}=2\times 10^{20}$ eV. The EBL used is from [69]. Twelve cascade cycles are sufficient to reach convergence, and this is the number used to calculate the total Cen A spectral energy distribution induced by UHECRs interacting with intervening radiation fields. The synchrotron cascade radiation is colored blue. For the assumed magnetic field, the synchrotron flux is produced by $\gamma\gtrsim 10^{12}$ electrons and remains collimated. However, the Compton flux between ~1–100 TeV does not take into account the deflection of electrons. It should therefore be considered as an upper limit that could be reached if $B\lesssim 10^{-12}$ G.

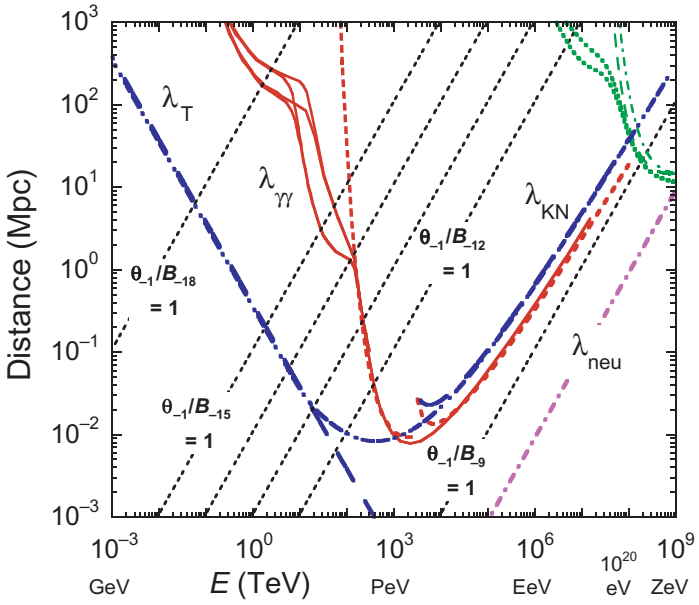

Figure 4. MFPs for attenuation of γ rays by the EBL ($\lambda_{\gamma\gamma}$), for Compton-scattering energy loss of relativistic electrons or positrons with the CMBR in the Thomson (λ_T) and Klein–Nishina (λ_{KN}) regimes, and neutron decay (λ_{neu}). The photopion energy-loss path length for protons, from figure 1, is shown for comparison. The particle or photon energy is denoted E(TeV). The short-dashed lines give length for a lepton to be deflected by $0.1\theta_{-1}$ rad in a magnetic field from 10^{-9} to 10^{-18} G, as labeled. Neutron decay length is given by λ_{neu}.

The solid curve in figure 5 shows the multiwavelength νF_ν flux, but is clearly far too faint to be seen with the present technology. In this case, the proximity of Cen A works against it being a bright hadronic source: there is not enough pathlength to extract a significant fraction of the UHECR proton's energy. In future work (Atoyan *et al* 2009, in preparation), details of cascades formed by UHE leptons and γ-rays formed by photohadronic processes will be presented. The prospects of detecting more distant, aligned blazar jets, if they are sources of UHECRs, could be more favorable if $B \lesssim 10^{-12}$ G. UHECR production in luminous flat spectrum radio quasars could make anomalous hard components at multi-GeV energies to be detected with the Fermi Gamma ray Space Telescope. Such emission signatures could also be seen in GRBs [70, 71].

6. Summary and conclusions

We have considered the implications of the discovery [1, 2] by the Pierre Auger Collaboration of clustering of UHECR arrival directions towards Cen A and AGN in the SGP. To guide our thinking, we have introduced a model-independent definition of the GZK horizon distance, shown in figure 2 (cf [18, 19]). Assuming that black-hole jets energize and inflate the radio lobes of radio galaxies, a new method to calculate jet power based on the radio spectrum, size, and jet/counterjet ratio is applied to Cen A data. The average absolute jet power of Cen A is found from this technique to be $\approx 10^{44}$ erg s^{-1}. The apparent isotropic power in a small beaming cone could easily, therefore, exceed 10^{46} erg s^{-1} during flaring intervals.

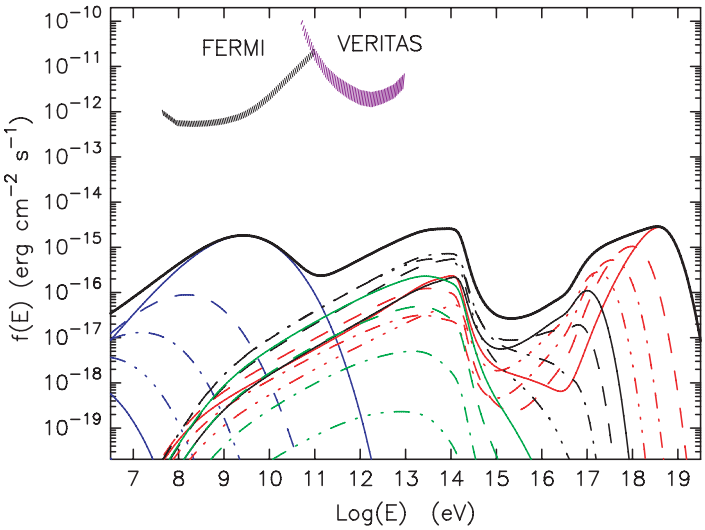

Figure 5. Rectilinear cascade formed by photohadronic processes from UHECRs produced by Cen A. Lower-energy blue family of curves shows the synchrotron emission from successive generations of the cascade, and higher-energy red family shows various generations of the Compton/γ–γ cascade. One-year Fermi Gamma ray Space Telescope/GLAST and 50 h VERITAS sensitivities are shown for comparison.

An apparent jet power at least this great is needed to accelerate UHECRs through Fermi processes. The collimated UHECRs, consisting mainly of neutron-decay protons, can be deflected by the $\approx\mu$G fields in the lobes of radio galaxies (for acceleration in the lobes of radio galaxies see e.g. [72]). This can give the appearance that UHECRs are emitted from Cen A's radio lobes [28], or allow UHECRs to originate from more distant, misaligned radio galaxies like Cyg A, which itself has a highly magnetized, $\approx$20 μG cavity within several hundred kpc of the central engine [31]. The enhancement of UHECRs in the directions to specific radio jet sources at different redshifts would give valuable information about the IGM magnetic fields and the intensity of the EBL.

The inner jets of radio galaxies, including Cen A, can make an escaping neutral beam of UHECRs. Because Cen A is a nearby radio galaxy with its closer jet misaligned by $\sim$35°–70° to the line of sight, the UHECR flux received from it is small, and the cascade radiation flux is not detectable with current instrumentation. Neither is the secondary nuclear γ-ray emission from cosmic ray interactions with the lobe's thermal gas if its density is $\approx 10^{-4}$ cm^{-3} [47], though the pair halo flux could be detectable [73, 74]. The most prominent multi-MeV radiation signature is due to the CMB photons Compton-scattered by the radio-emitting electrons to soft γ-ray energies [47, 66]. The use of the transient event class in the analysis of Cen A data [75] could help pull out the low-energy, $\approx$10–100 MeV signal, which would be important for normalizing its magnetic field and total jet power.

For UHECR blazar sources pointed towards us, anomalous hard cascade γ radiation spectra is potentially detectable with the Fermi Gamma ray Space Telescope or ground-based γ-ray telescopes, as we show in detail in future work. The detection of anomalous γ-ray signatures in blazars (or GRBs) could reveal emissions from UHECR acceleration in these sources. Lack

of association of UHECR arrival directions with radio galaxies could require that various other classes of extragalactic bursting sources be admitted, including long duration GRBs [76, 77], low luminosity GRBs [78], or magnetars. For instance, Ghisellini *et al* [79] argue that the Auger UHECRs are not actually associated with Cen A, but with the background Centaurus cluster at ≈40–50 Mpc. They argue that the rapid discharge of young, highly magnetized pulsars, which are the progenitors of magnetars, might have sufficient power to explain UHECRs' origin. Here the future pattern of UHECR arrival directions found with the Pierre Auger Observatory is of great interest, and whether a concentration builds toward the direction to Cen A.

Spectral signatures associated with UHECR hadron acceleration in studies of radio galaxies and blazars with the Fermi Gamma ray Space Telescope and ground-based γ-ray observatories can provide evidence for cosmic-ray particle acceleration in black-hole plasma jets. Together with IceCube or a northern hemisphere neutrino telescope, observations of PeV neutrino and MeV–GeV–TeV γ rays can confirm whether black-hole jets in radio galaxies accelerate the UHECRs.

Acknowledgments

Useful discussions and correspondence with Roger Blandford, Teddy Cheung, Diego Harari, Vasiliki Pavlidou, Esteban Roulet, and Alan Watson are gratefully acknowledged. We thank Dr Floyd Stecker for alerting us to an error in the calculations of the photopion losses of protons in the EBL. Visits of AA to the Naval Research Laboratory and the research of JDF are supported by NASA GLAST Interdisciplinary Science Investigation Grant DPR-S-1563-Y. The research of CD is supported by the Office of Naval Research.

References

[1] Auger Collaboration 2007 *Science* **318** 939
[2] The Pierre Auger Collaboration 2008 *Astropart. Phys.* **29** 188
[3] Watson A A 2008 arXiv:0801.2321
[4] Yamamoto T (The Pierre Auger Collaboration) 2007 arXiv:0707.2638
Abraham J *et al* 2008 *Phys. Rev. Lett.* **101** 061101
[5] Unger M, Engel R, Schüssler F, Ulrich R and Pierre Auger Collaboration 2007 *Astron. Nachrichten* **328** 614
[6] Sokolsky P 2008 private communication
[7] Unger M, Dawson B R, Engel R, Schüssler F and Ulrich R 2008 *Nucl. Instrum. Methods Phys. Res.* A **588** 433
[8] Engel R (The Pierre Auger Collaboration) 2007 arXiv:0706.1921
[9] Véron-Cetty M-P and Véron P 2006 *Astron. Astrophys.* **455** 773
[10] Alvarez-Muñiz J, Engel R and Stanev T 2002 *Astrophys. J.* **572** 185
[11] Waxman E 1995 *Phys. Rev. Lett.* **75** 386
[12] Waxman E and Coppi P 1996 *Astrophys. J. Lett.* **464** L75
[13] Dermer C D 2007 *30th ICRC (Mérida, Yucatan, Mexico)* (arXiv:0711.2804)
[14] HiRes Collaboration 2007 (arXiv:astro-ph/0703099)
HiRes Collaboration 2008 *Phys. Rev. Lett.* **100** 101101
[15] Greisen K 1966 *Phys. Rev. Lett.* **16** 748
[16] Zatsepin G T and Kuz'min V A 1966 *JETP Lett.* **4** 78
[17] Stanev T, Engel R, Mücke A, Protheroe R J and Rachen J P 2000 *Phys. Rev.* D **62** 093005
[18] Harari D, Mollerach S and Roulet E 2006 *J. Cosmol. Astropart. Phys.* JCAP11(2006)012

[19] Lu C-C and Lin G-L 2008 arXiv:0804.3122
[20] Taylor A M and Aharonian F A 2008 *Phys. Rev.* D submitted (arXiv:0811.0396)
[21] Abbasi R U *et al* 2008 arXiv:0804.0382
[22] Stanev T, Biermann P L, Lloyd-Evans J, Rachen J P and Watson A A 1995 *Phys. Rev. Lett.* **75** 3056
[23] Stecker F W 1968 *Phys. Rev. Lett.* **21** 1016
[24] Shaver P A and Pierre M 1989 *Astron. Astrophys.* **220** 35
[25] Wall J V and Peacock J A 1985 *Mon. Not. R. Astron. Soc.* **216** 173
[26] Stanev T 2008 arXiv:0805.1746
[27] George M R, Fabian A C, Baumgartner W H, Mushotzky R F and Tueller J 2008 *Mon. Not. R. Astron. Soc.* **388** L59
[28] Moskalenko I V, Stawarz L, Porter T A and Cheung C C 2009 *Astrophys. J.* at press arXiv:0805.1260
[29] Zaw I, Farrar G R and Greene J E 2008 arXiv:0806.3470
[30] Molina M *et al* 2007 *Mon. Not. R. Astron. Soc.* **382** 937
[31] Atoyan A and Dermer C D 2008 *Astrophys. J. Lett.* **687** L75
Cheung C C 2008 private communication
[32] Nagar N M and Matulich J 2008 *Astron. Astrophys.* **488** 879
[33] Alvarez H, Aparici J, May J and Reich P 2000 *Astron. Astrophys.* **355** 863
[34] Ebneter K and Balick B 1983 *Publ. Astron. Soc. Pac.* **95** 675
[35] Gu Q, Maiolino R and Dultzin-Hacyan D 2001 *Astron. Astrophys.* **366** 765
[36] Zhang E-P and Wang J-M 2006 *Astrophys. J.* **653** 137
[37] Atoyan A and Dermer C D 2001 *Phys. Rev. Lett.* **87** 221102
[38] Atoyan A M and Dermer C D 2003 *Astrophys. J.* **586** 79
[39] Georganopoulos M and Kazanas D 2003 *Astrophys. J. Lett.* **594** L27
[40] Ghisellini G and Tavecchio F 2008 *Mon. Not. R. Astron. Soc.* **386** L28
[41] Finke J D, Dermer C D and Böttcher M 2008 *Astrophys. J.* **686** 181
[42] Kraft R P, Forman W R, Jones C, Murray S S, Hardcastle M J and Worrall D M 2002 *Astrophys. J.* **569** 54
[43] Hardcastle M J, Worrall D M, Kraft R P, Forman W R, Jones C and Murray S S 2003 *Astrophys. J.* **593** 169
[44] Kinzer R L *et al* 1995 *Astrophys. J.* **449** 105
[45] Sreekumar P, Bertsch D L, Hartman R C, Nolan P L and Thompson D J 1999 *Astropart. Phys.* **11** 221
[46] Gupta N 2008 *J. Cosmol. Astropart. Phys.* JCAP06(2008)022
[47] Hardcastle M J, Cheung C C, Feain I J and Stawarz L 2008 arXiv:0808.1593
[48] Cuoco A and Hannestad S 2007 arXiv:0712.1830
[49] Waxman E and Bahcall J 1999 *Phys. Rev.* D **59** 023002
[50] Dermer C D and Menon G 2009 *High Energy Radiation from Black Holes* (Princeton, NJ: Princeton University Press) to be published
[51] Mirabel I F and Rodríguez L F 1998 *Nature* **392** 673
[52] Atoyan A M and Aharonian F A 1997 *Astrophys. J. Lett.* **490** L149
[53] Rawlings S and Saunders R 1991 *Nature* **349** 138
[54] Skibo J B, Dermer C D and Kinzer R L 1994 *Astrophys. J. Lett.* **426** L23
[55] Aharonian F *et al* 2007 *Astrophys. J. Lett.* **664** L71
[56] Asada K, Kameno S, Shen Z-Q, Horiuchi S, Gabuzda D C and Inoue M 2006 *Publ. Astron. Soc. Japan* **58** 261
[57] Dhawan V, Kellerman K I and Romney J D 1998 *Astrophys. J. Lett.* **498** L111
[58] Dermer C D 2008 *Astrophys. J.* **684** 430
[59] Sari R, Piran T and Narayan R 1998 *Astrophys. J. Lett.* **497** L17
[60] Horiuchi S, Meier D L, Preston R A and Tingay S J 2006 *Publ. Astron. Soc. Japan* **58** 211
[61] Virmani A, Bhattacharya S, Jain P, Razzaque S, Ralston J P and Mckay D W 2002 *Astropart. Phys.* **17** 489
[62] Hayashida N *et al* 1999 *Astrophys. J.* **522** 225
[63] Dermer C D 1986 *Astrophys. J.* **307** 47

[64] Sreekumar P *et al* 1998 *Astrophys. J.* **494** 523
[65] Kachelriess M, Ostapchenko S and Tomas R 2008 arXiv:0805.2608
[66] Cheung C C 2007 *1st GLAST Symp.* **921** 325
[67] Inoue S, Aharonian F A and Sugiyama N 2005 *Astrophys. J. Lett.* **628** L9
[68] Gabici S and Aharonian F A 2005 *Phys. Rev. Lett.* **95** 251102
[69] Primack J R, Bullock J S and Somerville R S 2005 *High Energy Gamma-Ray Astron.* **745** 23
[70] Dai Z G and Lu T 2002 *Astrophys. J.* **580** 1013
[71] Razzaque S, Mészáros P and Zhang B 2004 *Astrophys. J.* **613** 1072
[72] Fraschetti F and Melia F 2008 *Mon. Not. R. Astron. Soc.* **391** 1100
[73] Aharonian F A, Coppi P S and Voelk H J 1994 *Astrophys. J. Lett.* **423** L5
[74] Stawarz Ł, Aharonian F, Wagner S and Ostrowski M 2006 *Mon. Not. R. Astron. Soc.* **371** 1705
[75] Fermi Collaboration Atwood W *et al* 2009 *Astrophys. J.* submitted
[76] Wick S D, Dermer C D and Atoyan A 2004 *Astropart. Phys.* **21** 125
[77] Murase K, Ioka K, Nagataki S and Nakamura T 2008 *Phys. Rev.* D **78** 023005
[78] Wang X-Y, Razzaque S, Mészáros P and Dai Z-G 2007 *Phys. Rev.* D **76** 083009
[79] Ghisellini G, Ghirlanda G, Tavecchio F, Fraternali F and Pareschi G 2008 *Mon. Not. R. Astron. Soc.* **390** L88